

ROTATIONAL VELOCITIES OF B STARS

HELMUT A. ABT

Kitt Peak National Observatory, P.O. Box 26732, Tucson, AZ 85726-6732; abt@noao.edu

AND

HUGO LEVATO AND MONICA GROSSO

Complejo Astronomico El Leoncito, Casilla de Correo 467, 5400 San Juan, Argentina; hlevato@casleo.gov.ar

Received 2001 December 8; accepted 2002 March 10

ABSTRACT

We measured the projected rotational velocities of 1092 northern B stars listed in the Bright Star Catalogue (BSC) and calibrated them against the 1975 Slettebak et al. system. We found that the published values of B dwarfs in the BSC average 27% higher than those standards. Only 0.3% of the stars have rotational velocities in excess of two-thirds of the breakup velocities, and the mean velocity is only 25% of breakup, implying that impending breakup is not a significant factor in reducing rotational velocities. For the B8–B9.5 III–V stars the bimodal distribution in V can be explained by a set of slowly rotating Ap stars and a set of rapidly rotating normal stars. For the B0–B5 III–V stars that include very few peculiar stars, the distributions in V are not bimodal. Are the low rotational velocities of B stars due to the occurrence of frequent low-mass companions, planets, or disks? The rotational velocities of giants originating from late B dwarfs are consistent with their conservation of angular momentum in shells. However, we are puzzled by why the giants that originate from the early B dwarfs, despite having 3 times greater radii, have nearly the same rotational velocities. We find that all B-type primaries in binaries with periods less than 2.4 days have synchronized rotational and orbital motions; those with periods between 2.4 and 5.0 days are rotating within a factor 2 of synchronization or are “nearly synchronized.” The corresponding period ranges for A-type stars are 4.9 and 10.5 days, or twice as large. We found that the rotational velocities of the primaries are synchronized earlier than their orbits are circularized. The maximum orbital period for circularized B binaries is 1.5 days and for A binaries is 2.5 days. For stars of various ages from $10^{7.5}$ to $10^{10.2}$ yr the maximum circularized periods are a smooth exponential function of age.

Subject headings: binaries: spectroscopic — diffusion — stars: early-type — stars: peculiar — stars: rotation

On-line material: machine-readable table

1. INTRODUCTION

The rotational velocities of B stars listed in the Bright Star Catalogue (BSC; Hoffleit & Jaschek 1982) come from a variety of sources that have been calibrated against different standards. That makes it difficult to use those velocities for statistical studies. Therefore, we decided to measure the rotational velocities of all the B stars that could easily be reached from Kitt Peak on a uniform system that is calibrated against the most recent Slettebak standards (Slettebak et al. 1975). What was measured for each star was the FWHM of the observed absorption line profiles of $\lambda 4471$ He I and $\lambda 4481$ Mg II. Figure 1 of Abt & Morrell (1995) shows that such measures work even down to small values of $V \sin i$ such as 10 km s^{-1} . These yielded a mean projected rotational velocity, $V \sin i$, where V is the equatorial linear rotational velocity and i is the angle between the rotational axis and light of sight. We observed virtually all of the B stars between declinations -30° and $+70^\circ$, namely, 1092 stars. Once those measures were made, we could explore the correlations with spectral peculiarities, evolutionary tracks, and duplicity.

2. OBSERVATIONAL DATA

The stars were selected from both the third (Hoffleit 1964) and fourth (Hoffleit & Jaschek 1982) editions of the BSC

because we did not wish to overlook stars, such as Ap and B9.5p, that changed from A to B stars between editions. Each star was observed once with the Kitt Peak 0.9 m coudé feed telescope and 2.1 m coudé spectrograph. We used a $304 \text{ mm} \times 361 \text{ mm}$ grating having $632 \text{ grooves mm}^{-1}$ to illuminate a Tek CCD with $800 \text{ pixels} \times 800 \text{ pixels}$ of size 0.015 mm . The reciprocal dispersion was 7.0 \AA mm^{-1} and the resolution was 0.11 \AA or 7.1 km s^{-1} . These give a spectral range of 84 \AA in the single order observed. The spectra were flat-fielded, and thorium-argon hollow-cathode discharge tube spectra were added for wavelength calibration. The reductions were made with the IRAF program. The $\lambda 4471$ and 4481 profiles were fitted to Lorentzian or Gaussian profiles to yield the equivalent widths (EWs) and the FWHMs of both lines wherever possible. Some of the B9p and B9.5p spectra had too weak $\lambda 4471$ to measure, and $\lambda 4481$ was too weak in some early B stars. In all cases the measurements were checked against paper copies of the spectra.

We calibrated our line widths against Slettebak et al. (1975) standards. That was done for 44 stars in common having values of $V \sin i$ between less than 10 and 320 km s^{-1} . Our values of $V \sin i = 0.996(V \sin i)_{\text{SCBWP}} + 0.2 \text{ km s}^{-1}$, where SCBWP refers to the Slettebak et al. values. The mean scatter was $\pm 17.2 \text{ km s}^{-1}$, so that is a measure of our accuracy per star. Actually, the error is a function of $V \sin i$, being ± 9.0 , ± 16.1 , and $\pm 24.1 \text{ km s}^{-1}$ for $V \sin i < 50$, 50–150, and greater than 150 km s^{-1} , respectively. We also com-

pared our measures for 110 stars observed both by Abt & Morrell (1995) and here. They were mostly Ap stars, but the total set had $0 \text{ km s}^{-1} < V \sin i < 295 \text{ km s}^{-1}$. The mean difference is $(V \sin i)_{\text{ALG}} = (V \sin i)_{\text{AM}} - 1.3 \text{ km s}^{-1}$, and the random error per star is $\pm 21.0 \text{ km s}^{-1}$. We note that the latter error is close to the sum, added as squares, of the random error of $\pm 17.2 \text{ km s}^{-1}$ for the B stars and $\pm 8.9 \text{ km s}^{-1}$ for the A stars.

We can compare our results for the B and A stars with those of others. Abt & Morrell (1995) used the Slettebak et al. (1975) calibration for A stars with results that agree well with Wolff & Simon (1997), namely, $(V \sin i)_{\text{WS}} = 1.06(V \sin i)_{\text{AM}} - 4.4 \text{ km s}^{-1}$. Brown & Verschueren (1997), using several methods to derive rotational velocities, agree well with the Slettebak et al. (1975) standard for $V \sin i < 200 \text{ km s}^{-1}$. However, for five out of seven standards with $200 \text{ km s}^{-1} < V \sin i < 300 \text{ km s}^{-1}$, they found that the Slettebak values were too small by about 35 km s^{-1} .

On the other hand, Royer et al. (2002) have derived a new set of standards for B8–F2 stars using *Hipparcos* parallaxes, new model atmospheres, and measured rotational velocities derived with Fourier transforms. They find that the Slettebak et al. and the Abt & Morrell rotational velocities are too small, namely, $V \sin i = 1.04(V \sin i)_{\text{SCBWP}} + 6.1 \text{ km s}^{-1}$ and $V \sin i = 1.08(V \sin i)_{\text{AM}} + 5.3 \text{ km s}^{-1}$ for values greater than 25 km s^{-1} . These amount to +11 and +15 km s^{-1} , respectively, for typical dwarf rotational velocities of 120 km s^{-1} . We were tempted to adopt these new standards except that (1) they have not yet been derived for the B0–B7 stars and (2) the differences are smaller than our random error.

We also obtained a parallel set of spectra of 39 \AA mm^{-1} reciprocal dispersion with the 2.1 m Cassegrain spectrograph to resolve questions of classification and line strengths. We originally planned to obtain new MK classifications from these spectra but judged that the ones published in the BSC, obtained mostly by Morgan, Lesh, and other experienced classifiers, did not need to be repeated.

Our measurements are listed in Table 1, which is given in full only in the on-line edition. The successive columns give (1) the HR or BSC number, (2) the Henry Draper number because some other catalogs use this, (3) the spectral classification taken primarily from Hoffleit & Jaschek (1982), (4) the derived project rotational velocity averaged between the values obtained from $\lambda\lambda 4471$ and 4481 , (5) the equivalent width of $\lambda 4471$ in milliangstroms, (6) the equivalent width of $\lambda 4481$ in milliangstroms, and (7) comments. The comments tell which stars were Slettebak et al. standards (designated “rot. std.”), which stars have spectroscopic binary

orbits (SB10, SB20) in Batten, Fletcher, & MacCarthy (1989), specific star identifications in doubles, and comments about the line character (n = broad, s = sharp).

3. RESULTS

3.1. Mean Rotational Velocities

The mean values of $V \sin i$ for all stars with published luminosity classes are listed in Table 2. The entries in the table give values of $V \sin i$, the standard error in those means, and the numbers of stars (in parentheses) represented in the means. Although Ap stars have smaller rotational velocities than normal stars, the spectral appearance is the result of their low rotational velocities, not the cause of those velocities (Michaud 1980). Therefore, all peculiar stars should be included at this stage of the analysis, although we will discuss them separately below. The values of $V \sin i$ are grouped together for several spectral types to increase the accuracy in the means. This is justified because the means change slowly with type.

We will not discuss here the bright giants (class II) and supergiants (class I). They have large but systematic contributions from atmospheric turbulence. We cannot add to the discussion by Abt (1957, 1958).

The mean rotational velocities seem to go through slight peaks at about B8 V (or later), B7 IV, and B3 III.

3.2. Rotational Velocities in the BSC

The published rotational velocities in the BSC (Hoffleit & Jaschek 1982) are large compared with the Slettebak et al. (1975) standards. Linear least-squares comparisons for stars of all luminosity classes give

$$\text{B0–B9} : (V \sin i)_{\text{BSC}} = 1.103(V \sin i)_{\text{SCBWP}} + 16.5 \text{ km s}^{-1} \\ (131 \text{ stars}), \quad (1)$$

$$\text{A0–A9} : (V \sin i)_{\text{BSC}} = 1.030(V \sin i)_{\text{SCBWP}} + 10.4 \text{ km s}^{-1} \\ (56 \text{ stars}), \quad (2)$$

$$\text{F0–F9} : (V \sin i)_{\text{BSC}} = 1.193(V \sin i)_{\text{SCBWP}} + 2.5 \text{ km s}^{-1} \\ (27 \text{ stars}). \quad (3)$$

For an average rotational velocity of 100, 100, and 50 km s^{-1} for the B, A, and F stars, respectively, the BSC velocities are 27%, 13%, and 24% higher than Slettebak et al. standards.

TABLE 1
ROTATIONAL VELOCITIES AND EQUIVALENT WIDTHS OF B STARS

HR (1)	HD (2)	Spectral Type (3)	$V \sin i$ (km s^{-1}) (4)	EW($\lambda 4471$) (m\AA) (5)	EW($\lambda 4481$) (m\AA) (6)	Comments (7)
7.....	144	B9 IIIe	120	570	530	
15.....	358	B8 IVpMnHg	50	140	130	SB10
16.....	360	B9 Vn	240	140	230	
28.....	584	B7 IV	15	590	350	
38.....	829	B2 V	0	990	170	

NOTE.—Table 1 is published in its entirety in the electronic edition of the *Astrophysical Journal*. A portion is shown here for guidance regarding its form and content.

TABLE 2
MEAN PROJECTED ROTATIONAL VELOCITIES FOR ALL STARS WITH KNOWN LUMINOSITY CLASSES

TYPE	$\langle V \sin i \rangle, \sigma$ in the Mean (km s ⁻¹)				
	V	IV	III	II	I
B0–B2	127 ± 8 (134)	84 ± 10 (69)	111 ± 18 (29)	62 ± 21 (7)	69 ± 7 (23)
B3–B5	108 ± 8 (106)	94 ± 12 (43)	116 ± 19 (25)	65 ± 34 (5)	38 ± 2 (8)
B6–B8	152 ± 8 (128)	120 ± 14 (36)	74 ± 6 (105)	36 ± 9 (8)	52 ± 10 (6)
B9–B9.5	134 ± 7 (145)	99 ± 14 (30)	77 ± 8 (70)	20 ± 0 (3)	26 ± 2 (5)

NOTE.—Numbers in parentheses are numbers of stars represented in the means.

Royer et al. (2002) found that their new calibration for B8–F2 stars, mostly on the main sequence, gives values about 11% higher than Slettebak et al. standards, which is close to the above 13% for A stars. However, we have no information as to whether or not their later work will agree with the rotational velocities of the B and F stars in the BSC.

3.3. The Highest Rotational Velocities of the B Stars

We are used to thinking that many of the B stars have very broad lines, but we found only 26 stars (2.4%) with $V \sin i \geq 300$ km s⁻¹ and three stars (0.3%) with $V \sin i \geq 350$ km s⁻¹. The highest projected velocity for any luminosity class is 410 km s⁻¹ for HR 496 = ϕ Per. For that star, Slettebak (1966) derived a rotational velocity of 450 km s⁻¹, and that is the largest rotational velocity that he found for B stars. As he pointed out, that is 85% of the equatorial breakup velocity. We find only three stars having rotational velocities greater than two-thirds of the breakup velocities. The average rotational velocity of 130 km s⁻¹ is only one-quarter of the breakup velocity. Therefore, impending breakup is not a limiting factor for the rotational velocities of most B stars.

The results for A stars (Abt & Morrell 1995) are similar. Only six stars (0.4%) have $V \sin i \geq 300$ km s⁻¹, which is 70% of breakup. A rough average of 100 km s⁻¹ for A stars of luminosity classes III–V is only 25% of the equatorial breakup velocity. The rotational velocities of most A stars are not determined by impending breakup.

3.4. Ap Stars and the Bimodal Distribution in B8–B9.5 Rotational Velocities

Michaud (1980) showed that if a late B or A star has an equatorial rotational velocity of less than about 120 km s⁻¹, diffusion will occur in an outer convection zone, and the atmosphere will become rich in some elements and depleted in others. The abundance patterns resemble those of Ap and Am stars. Conversely, if the star is a rapid rotator, it will remain well mixed, and its spectrum will show a normal composition. Abt (2000) argued that among A stars the distribution of equatorial rotational velocities can be simulated by populations of slowly rotating abnormal stars and rapidly rotating normal stars. Does this apply to the late B stars, which include many Ap stars?

We considered the 453 B8–B9.5 III, IV, or V stars of all kinds (normal, Ap, emission line). Their values of $V \sin i$ give a distribution that has a peak at 50 km s⁻¹. That distribution was deconvolved assuming random orientations of axes, an assumption has been shown by Abt (2001) to be jus-

tified. The resulting distribution shown in Figure 1 is strongly bimodal. But which stars are the Ap stars and which are the normal ones because in deconvolving a statistical distribution we lose track of individual stars?

The Ap stars are often evolved to the upper edge of the main sequence; they often have luminosity classes of III or IV because it takes 10⁷ yr to form Ap(HgMn) stars and nearly 10⁸ yr to form Ap(SrCr) stars (Abt 1979; Hubing, North, & Mathys 2000). They all have $V \sin i < 150$ km s⁻¹, so they all fall in the left peak of Figure 1. However, that peak contains 241 stars, and only 121 of them are Ap stars (mostly HgMn). What are the remaining 120 stars?

Visual spectral classification does not always discover all the abnormal stars unless the classification is done very critically. Consider the distribution of EWs of $\lambda 4481$ Mg II shown in Figure 2 for 119 B8 III–V normal and 21 B8 Ap stars. We see in the top panel that all 27 of the Ap stars have low values of EW, namely, less than 340 mÅ. That is consistent with the results for the A stars (Abt & Morrell 1995) where all the Ap stars have EW($\lambda 4481$) in the low half of its range, namely, less than 400 mÅ. Of the remaining B stars in Figure 2, those with $V \sin i > 120$ km s⁻¹ and therefore $V > 120$ km s⁻¹ should be normal stars according to Michaud’s criterion. For random orientation of rotational axes and for an average $V = 200$ km s⁻¹, 80% should have $V \sin i > 120$ km s⁻¹ and 20% should have $V \sin i < 120$ km s⁻¹. If the former represents the 63 stars in the right half of

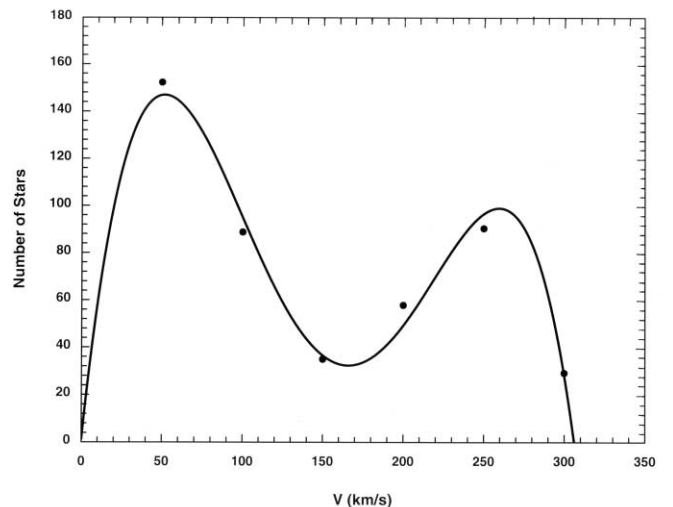


FIG. 1.—For 453 B8–B9.5 III, IV, and V stars we have deconvolved the distribution in $V \sin i$ into this one in V .

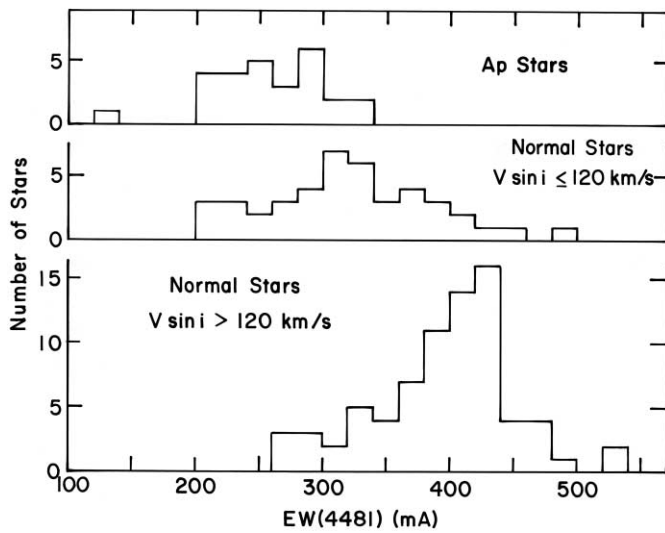


FIG. 2.—Top panel shows the distribution of equivalent widths of $\lambda 4481$ Mg II in 27 B8p–B9.5p stars. The middle panel represents the distribution of equivalent widths of $\lambda 4481$ in 43 normal B8–B9.5 stars having $V \sin i \leq 120 \text{ km s}^{-1}$. The bottom panel represents 76 normal B8–B9.5 stars with $V \sin i > 120 \text{ km s}^{-1}$. The text notes that all the Ap stars have $\text{EW}(\lambda 4481) < 340 \text{ m}\text{\AA}$. All the stars with $\text{EW}(\lambda 4481) > 340 \text{ m}\text{\AA}$ are normal with high rotational velocities, but the ones at the right in the middle panel are statistically those with small values of $\sin i$. We suspect that the “normal stars” with $\text{EW}(\lambda 4481) < 340 \text{ m}\text{\AA}$ in the middle and bottom panels are actually undetected B8p–B9.5p stars because their Mg II lines are abnormally weak.

the bottom panel, then the 15 latter stars in the right half of the middle panel are rapid rotators seen nearly pole-on.

That leaves the “normal” stars with $\text{EW}(\lambda 4481) < 340 \text{ m}\text{\AA}$ to be explained. We suggest that those 28 stars with weak Mg II and $V \sin i < 120 \text{ km s}^{-1}$ are undetected peculiar stars because their Mg II lines are abnormally weak. If so, the total number of Ap stars is 55 or twice the original number (27) of obvious Ap stars. Returning now to an explanation of Figure 1, we conclude that the left peak can be attributed totally to Ap stars, either ones detected visually or ones with weak Mg II lines, and the right peak is the normal stars.

That explains the double peak for the B8–B9.5 stars and confirms the Michaud (1970) theory that separates the slowly rotating peculiar stars from the rapidly rotating normal stars. However, what happens to the distributions of rotational velocities of the B0–B7 stars? Consider all the B0–B2 III, IV, and V stars, namely, those with normal spectra, a few He-rich or He-poor stars, and many emission-line stars. It seems reasonable to group all those together because most of those characteristics (e.g., emission lines) are the result of their rotational velocities, not the cause of those rotational velocities. If their distribution of rotational velocities is deconvolved, we obtain the curve in Figure 3. Please note that the peak of very uncertain height at very small values of V is the result of a curve-fitting program. The distribution for the B3–B5 III, IV, and V stars is almost identical. However, the shape of those curves is very different than that in Figure 1 for the B8–B9.5 III, IV, and V stars.

We do not know what the distribution of rotational velocities of early B stars should be. There are very few He-rich and He-poor stars known, but that paucity may be due

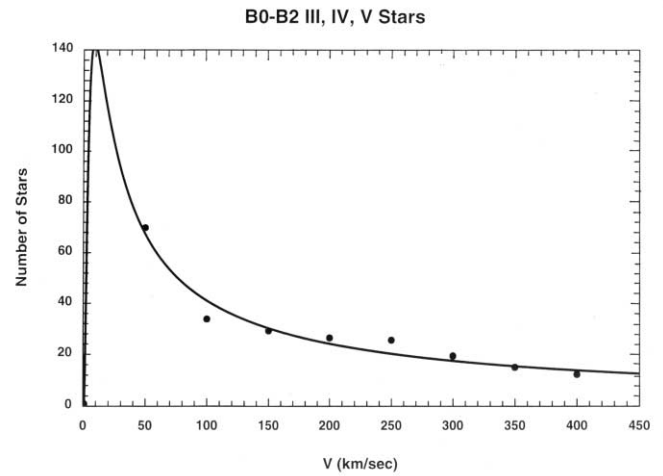


FIG. 3.—For 229 B0–B2 III, IV, and V stars we have deconvolved the distribution in $V \sin i$ into this one in V .

to an observational limitation. We considered using the measured values of $\text{EW}(\lambda 4471 \text{ He I})$ to identify others than the very extreme examples illustrated by Morgan and others; see Plate 12 of the atlas by Morgan, Abt, & Tapscott (1978). Stars such as HR 1851 and 1890 have 2–3 times stronger He I lines than normal stars. It would seem likely that there exist many less-extreme stars. But moderate examples of abnormal helium abundances are unlikely to be identified from classification spectra because the strengths of the helium lines are used to determine the spectral types. If a star has a moderate underabundance of helium, visual spectral classification will cause a later or earlier type, depending on which side of the helium peak strength at B3 the star occurs. What is needed is a reddening-free determination of effective temperatures for many B stars, such as has been done from spectrophotometric studies of a few B stars, that are independent of spectral classification; then the use of the $\text{EW}(\lambda 4471)$ measures would identify the moderate abnormalities. Colors, particularly in the infrared, may not be suitable because of the existence of disks or faint companions.

We also wondered about the affect of tidal breaking in close binaries toward reducing rotational velocities. A sample of B2–B5 IV or V stars that was studied for duplicity, independent of their lines widths, is given by Abt, Gomez, & Levy (1990). That is more reliable for statistical studies because B binaries in compilations such as that of Batten, Fletcher, & MacCarthy (1989) are heavily biased toward sharp-lined stars. One might suppose that occurrence in close binaries (periods < 10 days) would cause reduced rotational velocities, but (1) B binaries with $P = 3$ days, for instance, have synchronous rotational velocities of about 150 km s^{-1} and (2) the mean value of the deconvolved V for the Abt et al. binaries with $P < 10$ days is 125 km s^{-1} . Both those two values of V are close to the average for nonbinary stars. Therefore, the occurrence of some close binaries does not distort the distributions of rotational velocities. However, we do not know the frequency of occurrence of faint companions, disks, and planets that, like in the solar system, absorb most of the angular momentum. At present, our ability to discover companions to early B primaries is limited to $\geq 1 M_{\odot}$ (Abt et al. 1990). We wonder whether the low rotational velocities of B stars might be due to many low-

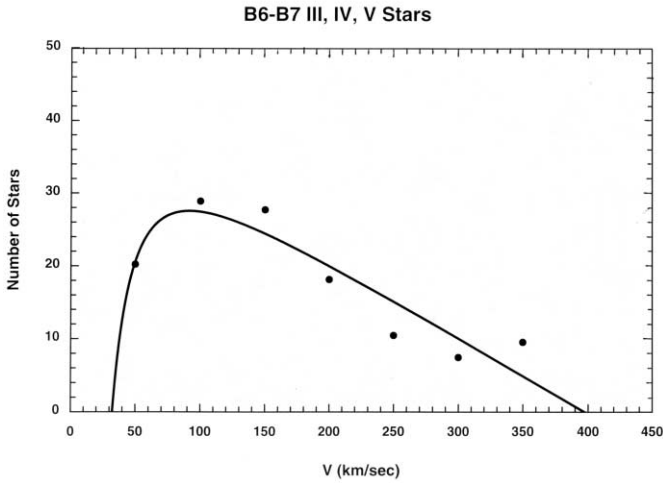


FIG. 4.—For 123 B6–B7 III, IV, and V stars we have deconvolved the distribution in $V \sin i$ into this one in V .

mass companions and disks, but we cannot test that hypothesis at this time.

Finally, we should comment on the B6–B7 III, IV, and V stars. The deconvolved distribution shown in Figure 4 for 123 such stars is intermediate between the strongly peaked distribution in Figure 3 for the B0–B2 stars and the double-peaked distribution in Figure 1 for the B8–B9 stars. In view of the likely classification errors of ± 1 spectral subclass, we should not expect a sharp demarcation between the two differing distributions.

3.5. Evolutionary Changes in Rotational Velocities

As dwarf B stars evolve and expand to become giants, we would expect their mean rotational velocities to decrease. There have been studies (e.g., Oke & Greenstein 1954) of that problem. Those authors considered two extreme cases: case A in which the stars continue to rotate as rigid bodies so that the angular momentum must be redistributed within the star during evolution and case B where the angular momentum is conserved by each shell, implying that differential rotation will occur within the star. In case B the rotational velocities should decrease in proportion to the increases in radii. In case A the mass distribution within the stars must be computed in both initial and final states, but it leads to smaller decreases in photospheric rotational velocities.

We employed interior models by Maeder (1990) for the evolutionary track for a star of $15 M_{\odot}$, models by Bertelli et al. (1986) for smaller masses, and standard relations (Drilling & Landolt 2000) between astronomical and physical parameters of stars. In Table 3 we list dwarf and giant types (in the second column) for sample masses in solar masses (given in the first column). The third column gives the initial and final rotational velocities by interpolating in Table 2. The standard errors taken from the means in Table 2 are about $\pm 10 \text{ km s}^{-1}$. The final two columns give the predicted rotational velocities for the two Oke & Greenstein cases.

We see in Table 3 that case B (conservation in shells) will fit the measured rotational velocities of the giants of masses 3 and $2 M_{\odot}$ but that neither case will fit the rotational velocities of mass 15 and $6 M_{\odot}$ giants. The measured rotational velocities of giants, especially those of $15 M_{\odot}$, are too large for us to understand. We used *Hipparcos* parallaxes, which

TABLE 3

MASS (M_{\odot})	TYPE CHANGE	MEASURED ($V \sin i$) (km s^{-1})	PREDICTED ($V \sin i$) (km s^{-1})	
			Case A	Case B
15.....	O9.7 V \rightarrow B1.5 III	118 \rightarrow 114	77	40
6.....	B3.0 V \rightarrow B5.6 III	126 \rightarrow 94	81	43
3.....	B6.8 V \rightarrow A1.2 III	134 \rightarrow 55	80	42
2.....	A0.6 V \rightarrow F5.3 III	112 \rightarrow 25	70	36

are about 4 times their estimated errors for these B0–B2 V and III stars, to show that their mean radii increase by a factor of about 3.0. How can stars of $15 M_{\odot}$ expand by a factor of 3.0 but virtually retain their original rotational velocities? We have no answer at this time.

3.6. Synchronization of Rotational and Orbital Motions in Close Binaries

One would expect closely spaced binaries to have their rotational and orbital motions synchronized, i.e., $P_{\text{rot}} = P_{\text{orb}}$. Recent theoretical studies of synchronization have been done by Zahn (1977 and earlier) and Tassoul (1987). This topic has a long history. Unfortunately, there are too many uncertain parameters involved to predict numerical values of the limiting periods for synchronization. For instance, if binaries were formed by capture, does that occur before or after pre-main-sequence contraction? The trend toward synchronization would be more effective when the stars are larger relative to their separation. However, Levato (1976) showed that part of the effect occurred during a star's lifetime on the main sequence.

We collected data on 113 spectroscopic binaries with B primaries and with orbital elements listed in Batten et al. (1989) or Abt et al. (1990). We obtained *Hipparcos* parallaxes for 112 of those; one was negative. We corrected for reddening using *Hipparcos* *UBV* photometry, and we used bolometric corrections compiled by Drilling & Landolt (2000). These allowed us to compute the synchronous rotational velocities, namely, $V_{\text{syn}} = 2\pi R P_{\text{syn}}^{-1} = 50.58 R P_{\text{orb}}^{-1}$, where R is measured in solar radii and the periods are in days. This repeats some of the analyses done by Giurricin, Mardirossian, & Mezzetti (1984a, 1984b, 1984c), but with the advantages of rotational velocities derived with a consistent set of standards and with *Hipparcos* parallaxes.

In Figure 5 we show the ratio of the measured projected rotational velocities to the computed synchronous velocities as a function of orbital periods for 98 stars with periods less than 20 days. The upper left diagonal cutoff is explained in that the measured rotational velocities have an upper limit of about 400 km s^{-1} and the average value of R is about $5 R_{\odot}$; therefore, the maximum value of the ordinate is roughly $1.6 P_{\text{orb}}$. This gives a diagonal rough upper limit from the origin to an ordinate of 16 for a period of 10 days.

An enlargement of the lower left corner of Figure 5 is shown in Figure 6. We see that the primaries in the shortest-period binaries, certainly less than 1.9 days, are probably rotating synchronously, allowing for the projection factor of $\sin i$ that takes on values between 0 and 1. However, the upper limit of that limiting period depends on an error analysis. The error in the ordinates depends primarily on those

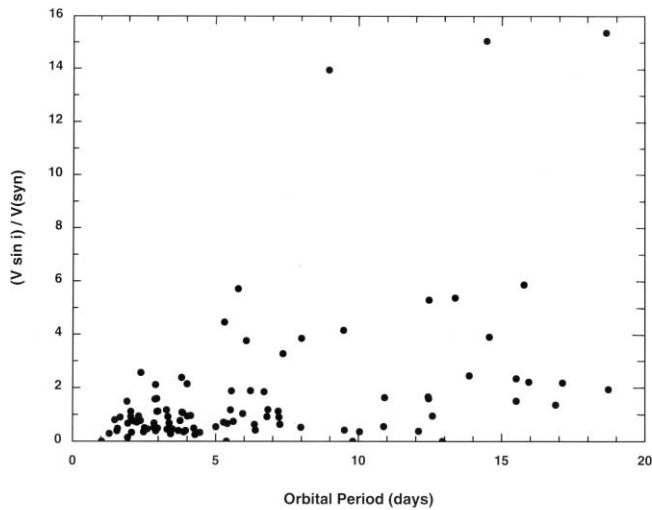


FIG. 5.—Ratios of the measured projected rotational velocities to their computed synchronous velocities are shown for 98 B-type binaries as a function of orbital period.

in two factors: $V \sin i$ and R . We can assume that the errors in the photometry, the tabulated effective temperatures and bolometric corrections, and the periods are negligible compared to those two. The mean error in $V \sin i$ is $\pm 17.2 \text{ km s}^{-1}$, compared with a mean rotational velocity for stars of luminosity classes V–III of 108 km s^{-1} ; that gives an estimated error of $\pm 16\%$. The estimated errors in the radii are directly proportional to the errors in the parallaxes; median values gives 27%. The combined error, added as squares, is $\pm 31\%$ in the ordinates. The mean value of $\sin i$ is $\pi/4$, so we would expect the ordinates for synchronized stars to be 0.79 ± 0.25 . The 18 stars with orbital periods less than 2.4 days have a mean ordinate of 0.65 ± 0.36 , which is in reasonable agreement with the expected values. Therefore, we conclude that the rotational and orbital motions are synchronized in all binaries with periods less than 2.4 days.

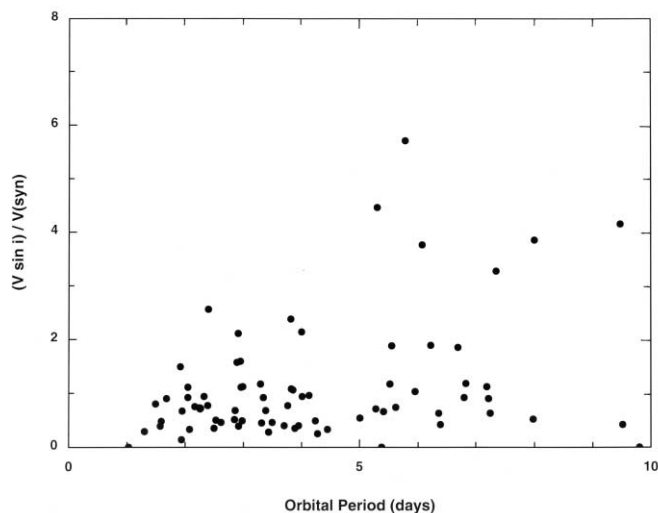


FIG. 6.—Enlargement of the lower left corner of Fig. 5. The text argues that the binaries with periods less than 2.4 days have primaries that are rotating synchronously with their orbital motions within their computation errors and allowing for various values of $\sin i$. Furthermore, the binaries with periods between 2.4 and 5 days are nearly synchronized.

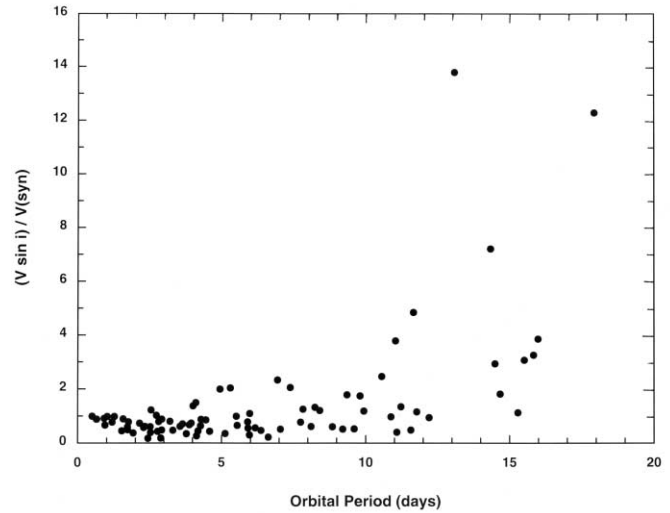


FIG. 7.—Ratios of the measured projected rotational velocities to the computed synchronous velocities are shown for 86 A-type primaries in orbits with periods less than 20 days.

What can we say about the 33 stars in binaries with periods of 2.4–5.0 days? On the average and allowing for similar errors, those stars are synchronized within a factor of 2. Therefore, we can say that they are “nearly synchronized.” The mean rotational velocity, $V \sin i$, of these primaries is low ($74 \pm 7 \text{ km s}^{-1}$) relative to single stars, but that may not be significant because the binaries listed in the Batten et al. (1989) compilation are mostly stars with sharp lines, i.e., low projected rotational velocities.

We can compare these results on synchronization with data on A-type binaries (Abt & Morrell 1995). Because A-type stars are older than B stars, they probably have had time to become synchronized to longer periods. We collected data, including *Hipparcos* parallaxes, for 134 binaries with orbital elements listed by Batten et al. and rotational velocities by Abt & Morrell. The ratios of the measured values of $V \sin i$ to the computed synchronous rotational velocities are given in Figure 7 for the 86 binaries with orbital periods up to 20 days. We see small values to 10.5 days and then strong deviations from synchronization for many binaries of longer periods.

Figure 8 is an enlargement of the lower left part of Figure 7. We suspect that the 42 binaries with periods less than 4.9 days might be synchronous. For these the mean value of the ratio is 0.70 ± 0.29 (s.e. per star), compared with expected values of 0.79 ± 0.15 . Therefore, all the binaries with periods less than 4.9 days seem to have their primaries rotating synchronously with their orbital motions. The 26 binaries with periods between 4.9 and 10.5 days have a mean value of the ratio of 1.07 ± 0.67 , indicating that on the average they have nearly synchronized motions. These period ranges are just twice those for the B stars, which are about a factor of 10 younger.

3.7. Circularization in Binaries

A second dynamical effect in close binaries is the gradual tendency for the orbits to become circular with time. In fact, Mathieu & Mazeh (1988) have suggested that the maximum orbital period for which all the binaries in a sample have circular orbits can be used as an approximate age determinant. In our present sample of B stars the ones with the

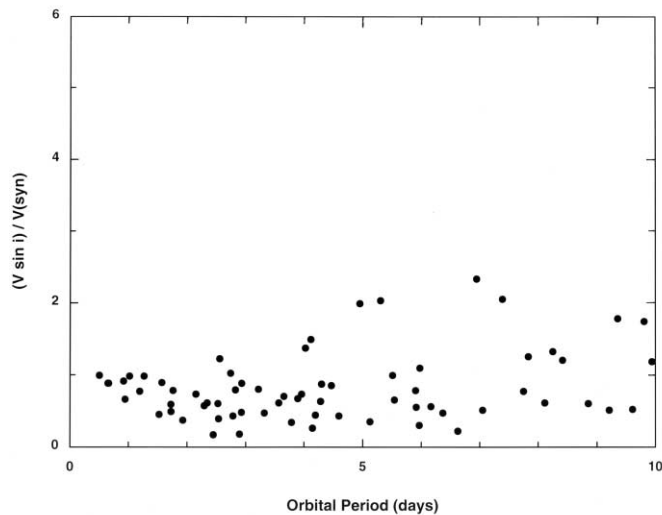


FIG. 8.—Enlargement of the lower left portion of Fig. 7. The text argues that within the measuring and computed errors and after allowing for various values of $\sin i$, the stars in binaries with periods less than 4.9 days are synchronized, while those with periods $4.9 \text{ days} < P < 10.5 \text{ days}$ are nearly synchronized.

shortest orbital periods and appreciable eccentricities are the B9.5 IV star HR 1221 = HD 24769 = 33 Tau with a period of 1.5919 days with $e = 0.37$ and the B1 V star HR 5944 = HD 143018 = π Sco with a period of 1.5701 days with $e = 0.15$. Therefore, 1.5 days is the limit for circularization.

For the A stars, the binary with the shortest period (2.5539 days) with $e > 0.10$ is the A1 Vp star HR 4380 = HD 98353 = 55 UMa. Its high eccentricity of 0.43 derived by Lloyd (1981) is convincing. He realized that this is the shortest period for a main-sequence primary with a large eccentricity. It is a double-lined system, but he could measure only the sharp-lined component. He concluded that the sharp-lined component is not rotating synchronously, although the broad-lined component is probably the more massive one. Abt & Morrell (1995) also stated that the broad-lined star is probably the primary. Using the *Hipparcos* parallax, the broad-lined star ($V \sin i = 65 \text{ km s}^{-1}$) is rotating synchronously, supporting the conclusion in the next paragraph.

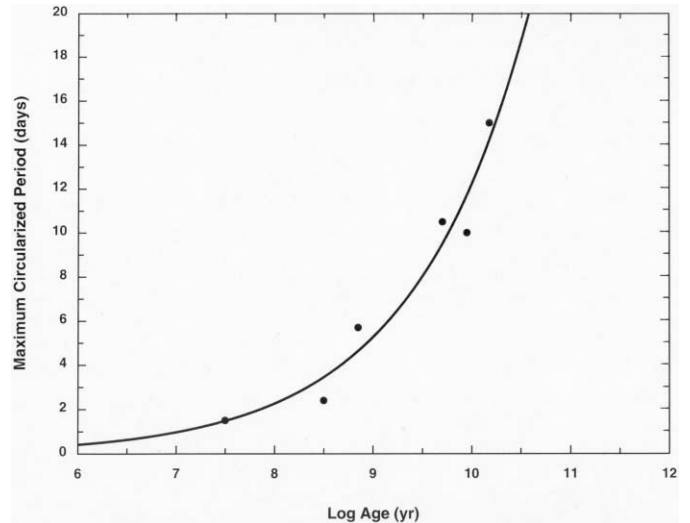


FIG. 9.—For various sets of stars, the maximum circularized periods are an exponential function of their ages. The left two data points represent B and A stars (III–V); the remaining data come from Duquennoy & Mayor (1991).

Note that whereas the longest synchronous periods are 2.4 and 4.9 days for the B and A stars, respectively, the longest periods that are circularized are 1.5 and 2.5 days, respectively. That must mean that synchronization of the primary rotational motion with the orbital motion occurs sooner than circularization of the orbits.

Duquennoy & Mayor (1991) have collected from the literature or their own work the data on the longest circularized periods for various groups of stars. Those are 5.7 days for the Hyades and Praesepe clusters, 10–11 days for M67 (from Mathieu & Mazeh 1988), more than 10 days for the old disk stars, and 12–19 days for halo stars (from Latham et al. 1988 and Jasniewicz & Mayor 1988). To these we add our two data points and ages from Allen (1963). The result is an exponential relation shown in Figure 9 that can be used, as Mathieu & Mazeh anticipated, to derive approximate ages for groups of coeval stars.

We thank John Landstreet for some good suggestions.

REFERENCES

- Abt, H. A. 1957, *ApJ*, 126, 503
 ———. 1958, *ApJ*, 127, 658
 ———. 1979, *ApJ*, 230, 485
 ———. 2000, *ApJ*, 544, 933
 ———. 2001, *AJ*, 122, 2008
 Abt, H. A., Gomez, A. E., & Levy, S. G. 1990, *ApJS*, 74, 551
 Abt, H. A., & Morrell, N. I. 1995, *ApJS*, 99, 135
 Allen, C. W. 1963, *Astrophysical Quantities* (2d ed.; London: Athlone), 264
 Batten, A. H., Fletcher, J. M., & MacCarthy, D. G. 1989, *Eighth Catalogue of the Orbital Elements of Spectroscopic Binary Systems* (Publ. Dom. Astrophys. Obs. Victoria 17; Victoria: Dominion Astrophys. Obs.)
 Bertelli, G., Bressan, A., Chiosi, C., & Angerer, K. 1986, *A&AS*, 66, 191
 Brown, A. G. A., & Verschueren, W. 1997, *A&A*, 319, 811
 Drilling, J. S., & Landolt, A. U. 2000, in *Allen's Astrophysical Quantities*, ed. A. N. Cox (4th ed.; New York: AIP), 381
 Duquennoy, A., & Mayor, M. 1991, *A&A*, 248, 485
 Giuricin, G., Mardirossian, F., & Mezzetti, M. 1984a, *A&A*, 131, 152
 ———. 1984b, *A&A*, 134, 365
 ———. 1984c, *A&A*, 135, 393
 Hoffleit, D. 1964, *Catalogue of Bright Stars* (3d rev. ed.; New Haven: Yale Univ. Obs.)
 Hoffleit, D., & Jaschek, C. 1982, *The Bright Star Catalogue* (4th rev. ed.; New Haven: Yale Univ. Obs.)
 Hubing, S., North, P., & Mathys, G. 2000, *ApJ*, 539, 352
 Jasniewicz, G., & Mayor, M. 1988, *A&A*, 203, 329
 Latham, D. W., Mazeh, T., Carney, B. W., McCrosky, R. E., Stefanik, R. P., & Davis, R. J. 1988, *AJ*, 96, 567
 Levato, H. 1976, *ApJ*, 203, 680
 Lloyd, C. 1981, *MNRAS*, 195, 805
 Maeder, A. 1990, *A&AS*, 84, 139
 Mathieu, R. D., & Mazeh, T. 1988, *ApJ*, 326, 256
 Michaud, G. 1970, *ApJ*, 160, 641
 ———. 1980, *AJ*, 85, 589
 Morgan, W. W., Abt, H. A., & Tapscot, J. W. 1978, *Revised MK Spectral Atlas for Stars Earlier than the Sun* (Yerkes Obs., Univ. Chicago, and Kitt Peak National Obs.)
 Oke, J. B., & Greenstein, J. L. 1954, *ApJ*, 120, 384
 Royer, F., Gerbaldi, M., Farragiana, R., & Gomez, A. E. 2002, *A&A*, 381, 105
 Slettebak, A. 1966, *ApJ*, 145, 126
 Slettebak, A., Collins, G. W., II, Boyce, P. B., White, N. M., & Parkinson, T. D. 1975, *ApJS*, 29, 137
 Tassoul, J.-L. 1987, *ApJ*, 322, 856
 Wolff, S. C., & Simon, T. 1997, *PASP*, 109, 759
 Zahn, J. P. 1977, *A&A*, 57, 383